9-2017

A Bioenergetics Systems Evaluation of Ketogenic Diet Liver Effects

Lewis J. Hutfles

Heather M. Wilkins

Scott J. Koppel

Ian W. Weidling

J. Eva Selfridge

See next page for additional authors

Authors

Lewis J. Hutfles, Heather M. Wilkins, Scott J. Koppel, Ian W. Weidling, J. Eva Selfridge, Eephie Tan, John P. Thyfault, Chad Slawson, Aron W. Fenton, Hao Zhu, and Russell H. Swerdlow

Published in final edited form as:

Appl Physiol Nutr Metab. 2017 September ; 42(9): 955–962. doi:10.1139/apnm-2017-0068.

A Bioenergetics Systems Evaluation of Ketogenic Diet Liver Effects

Lewis J. Hutfles[1,2], **Heather M. Wilkins**[2,3], **Scott J. Koppel**[2,4], **Ian W. Weidling**[2,4], **J. Eva Selfridge**[2,4], **Eephie Tan**[5], **John P. Thyfault**[4,6], **Chad Slawson**[5], **Aron W. Fenton**[5], **Hao Zhu**[5,7], and **Russell H. Swerdlow**[2,3,4,5,*]

[1]Kansas City University of Medicine and Biosciences, Kansas City, MO 64106

[2]University of Kansas Alzheimer's Disease Center, University of Kansas Medical Center, Kansas City, KS 66160

[3]Department of Neurology, University of Kansas Medical Center, Kansas City, KS 66160

[4]Department of Molecular and Integrative Physiology, University of Kansas Medical Center, Kansas City, KS 66160

[5]Department of Biochemistry and Molecular Biology, University of Kansas Medical Center, Kansas City, KS 66160

[6]Kansas City VA Medical Center, Kansas City, MO 64128

[7]Clinical Laboratory Sciences, University of Kansas Medical Center, Kansas City, KS 66150

Abstract

Ketogenic diets induce hepatocyte fatty acid oxidation and ketone body production. To further evaluate how ketogenic diets affect hepatocyte bioenergetic infrastructure, we analyzed livers from C57Bl/6J male mice maintained for one month on a ketogenic or standard chow diet. Compared to the standard diet, the ketogenic diet increased cytosolic and mitochondrial protein acetylation and also altered protein succinylation patterns. SIRT3 protein decreased while SIRT5 protein increased, and gluconeogenesis, oxidative phosphorylation, and mitochondrial biogenesis pathway proteins were variably and likely strategically altered. The pattern of changes observed can be used to inform a broader systems overview of how ketogenic diets affect liver bioenergetics.

Keywords

Bioenergetics; ketogenic diet; hepatocyte; liver; mitochondria

*Corresponding Author. University of Kansas Medical Center, MS 2012, 3901 Rainbow Blvd, Kansas City, KS 66160 USA. Tel.: 1-913-588-0970; fax 1-913-588-0681. rswerdlow@kumc.edu.

Conflict of Interest: The authors report no conflicts of interest associated with this manuscript.

Introduction

Diet manipulations can modify bioenergetic fluxes and the proteins that support those fluxes (Swerdlow 2014). Ketogenic diets, in particular, have robust effects. Ketogenic diets are high-fat, moderate protein, low carbohydrate diets that reduce insulin, spare glucose, and initiate and perpetuate ketone body production (Manninen 2004).

Ketogenic diets differ from high fat diet regimens that do not strictly minimize carbohydrates, and from low carbohydrate diets that substitute protein calories for carbohydrate calories. In the latter case, increasing gluconeogenic amino acid intake enhances glucose production, which in turn maintains insulin levels. If insulin does not fall, fatty acid mobilization and hepatocyte fatty acid oxidation do not initiate and robust ketosis does not occur.

Low insulin facilitates lipolysis and the carnitine palmitoyltransferase (CPT1a)-mediated import of fatty acids into hepatocyte mitochondrial matrices (Puchalska and Crawford 2017). This enables hepatocyte fatty acid oxidation and increases matrix acetyl CoA production. When acetyl CoA production rates exceed the capacity of citrate synthase (CS) to form citrate, or when oxaloacetate (OAA) levels are low, 3-hydroxy-3-methylglutaryl-CoA synthase 2 (HMGCS2) and 3-hydroxymethyl-3-methylglutaryl-CoA lyase (HMGCL) convert acetyl CoA to acetoacetate. Subsequent reduction of acetoacetate by D-beta-hydroxybutyrate dehydrogenase (BDH1) generates beta-hydroxybutyrate (Krebs et al. 1969; Lehninger et al. 1960; Newman and Verdin 2014), and acetoacetate also spontaneously decarboxylates to form acetone. These three ketone bodies enter the circulation via monocarboxylic acid (MCT) transporters, which allows acetoacetate and beta-hydroxybutyrate to access mitochondria in extrahepatic tissues and support respiration (Halestrap and Wilson 2012; Puchalska and Crawford 2017).

Ketogenic diets increase hepatic expression of fibroblast growth factor 21 (FGF21), peroxisome proliferator-activated receptor gamma (PPARγ), uncoupling protein 2 (UCP2), and CPT1a (Douris et al. 2015; Kennedy et al. 2007; McDaniel et al. 2011). They increase tricarboxylic acid metabolite levels and decrease catabolism pathways (Douris et al. 2015), increase β-oxidation-relevant gene expression, reduce lipid synthesis pathway expression, and inhibit the mechanistic target of rapamycin (mTOR) pathway (Kennedy et al. 2007; McDaniel et al. 2011). Ketogenic diets affect some post-translational protein modifications, including hepatocyte protein O-GlcNacylation and phosphorylation (Holland et al. 2016; Jornayvaz et al. 2010; McDaniel et al. 2011; Murata et al. 2013; Okuda et al. 2013).

How a ketogenic diet affects other particular bioenergetics-related pathways, though remains relatively unclear. In this study we analyzed the impact of a one-month ketogenic diet on liver proteins that facilitate specific bioenergetic pathways. Because the activity of bioenergetics-relevant proteins is frequently modified by post-translational modification, we screened the effects of a ketogenic diet on two directly relevant post-translational modifications, lysine acetylation and succinylation. We focused on lysine acetylation and succinylation, rather than other forms of post-translational modification, because ketogenic

diets directly affect acetyl CoA levels and because acetyl CoA and succinyl CoA can compete for lysine binding sites.

Materials and Methods

Animal procedures

Details of the mice used in this study and their handling are provided in a prior manuscript (Selfridge et al. 2015). Briefly, all animal procedures were approved by the University of Kansas Medical Center Animal Care and Use Committee, and we adhered to NIH guidelines for the proper treatment and use of laboratory animals. Twenty-six C57Bl/6J five-month old male mice (Jackson Laboratory, #000664) were placed on and subsequently completed a one-month ad libitum ketogenic (n=15) or standard chow (n=11) diet. The standard chow diet contained 3.0 kcal/g and the proportion of calories provided through that diet was 32% from protein, 14% from soybean oil fat, and 54% from carbohydrate (Teklad Harland rodent diet #8604). The ketogenic diet contained 7.2 kcal/g and the proportion of calories provided through that diet was 4.7% from protein, 93.4% from lard fat, and 1.8% from carbohydrate (BioServ #F3666). Ketosis in the ketogenic diet-fed mice was verified through measurements of serum β-hydroxybutyrate, which showed an approximate five-fold increase over that of the chow-fed mice (Selfridge et al. 2015).

Enrichment of liver mitochondria

120 mg of liver tissue, which had been frozen at the time each mouse was sacrificed, was thawed, minced, and washed in MSHE buffer (210mM mannitol, 70mM sucrose, 5 mM HEPES, 1mM EGTA, pH 7.4) with 0.5% bovine serum albumin (BSA). The tissue was homogenized using 10 strokes in a Dounce homogenizer in 5mL cold MSHE and centrifuged for 10 minutes at 800×g and 4°C. The supernatant was transferred to a new tube and again centrifuged for 10 minutes at 8000×g and 4°C. The resulting mitochondrial pellet was re-suspended in 500 μL of radioimmunoprecipitation assay (RIPA) lysis buffer (10mM Tris-Cl pH 8.0, 1mM EDTA, 0.5mM EGTA, 1% Triton X-100, 0.1% sodium deoxycholate, 0.1% SDS, and 140mM NaCl) with protease and phosphate inhibitors (Pierce, ThermoFisher).

Preparation of whole cell protein lysates

120 mg of frozen liver tissue was minced and washed in cold phosphate buffered saline (PBS). The tissue was homogenized with 10 strokes in a Dounce homogenizer in 1mL of RIPA lysis buffer containing protease and phosphatase inhibitors. The homogenate was centrifuged for 2 minutes in an Eppendorf 5417C centrifuge at 2,000 rpm and 4°C, and the supernatant was removed for subsequent use.

Immunochemistry

30 μg of protein lysate was separated by size via sodium dodecyl sulfate polyacrylamide gel electrophoresis (SDS-PAGE) using 4–15% Criterion TGX gels (Bio-Rad) and transferred to nitrocellulose membranes (Amersham Protran). Immunoblots were completed using the primary antibodies listed in Table 1. Secondary antibodies were purchased from Cell Signaling Technologies and used at a 1:2000 dilution. Immunoblots were visualized using

SuperSignal West Femto Maximum Sensitivity Substrate (ThermoFisher) on a ChemiDoc XRS platform (Bio-Rad).

Statistical and qualitative analyses

Lysine acetylation and succinylation blots were visually surveyed to identify inter-group changes in banding patterns, and to determine whether individual banding changes indicated increased or decreased staining. We did not perform quantitative densitometry on these blots.

Densitometry readings for the individual whole cell lysate proteins were quantitatively analyzed and normalized to the densitometry readings of the corresponding sample's tubulin band on the same blot. Densitometry readings for the enriched mitochondrial lysate densitometry were normalized to the corresponding sample's CS band on the same blot. To compare mean values of densitometry-analyzed proteins, F-tests were used to determine whether parameter variances were equivalent between the standard chow (n=11) and ketogenic diet (n=15) groups. If the F-test showed unequal variance a two-way non-parametric T-test was performed to determine the p value for the group means. If the F-test showed equivalent variance a two-way parametric T-test was used to determine the p value. P values less than 0.05 were considered significant.

Results

Proteome acetylation and succinylation, SIRT3, and SIRT5

Fatty acid oxidation rates impact acetyl CoA levels, which in turn influences substrate availability for acetylation modifications that can compete with succinylation modifications at protein lysine residues. We reasoned a ketogenic diet and elevation of fatty acid oxidation could alter lysine acetylation and succinylation patterns, and to test this we immunochemically screened whole cell and enriched mitochondrial lysates for changes in these post-translational modifications as well as enzymes that regulate these modifications. Figure 1A shows the degree of mitochondrial enrichment and purification that was achieved. Changes to the lysine acetylation pattern were evident both in enriched mitochondria (Figure 1B) and whole cell protein lysates (Figure 1C) from ketogenic diet fed mice, and the observed changes consistently indicated that the ketogenic diet caused increased acetylation. SIRT3, the major mitochondrial deacetylase, was decreased in both enriched mitochondria and whole cell protein lysates from ketogenic diet fed mice (Figure 1 B–D). Lysine succinylation levels did not appear to consistently change in one direction or another, although in both enriched mitochondria (Figure 1E) and whole cell protein lysates (Figure 1F) succinylation pattern changes were observed. SIRT5, a mitochondrial desuccinylase, was increased in enriched mitochondria but not whole cell protein lysates from ketogenic diet fed mice (Figure 1 E–G).

PDHC/PDHK1 and TCA cycle, glycolysis, and gluconeogenesis enzymes

We used densitometry to determine the whole cell protein lysate levels of pyruvate dehydrogenase complex subunits as well as tricarboxylic acid (TCA) cycle, glycolysis, and gluconeogenesis enzymes; enriched mitochondria protein samples were not used for these

analyses. In all cases densitometry values were normalized to those of tubulin and the resulting normalized values were used to make statistical comparisons.

Tubulin-normalized levels of a pyruvate dehydrogenase complex (PDHC) subunit, the pyruvate dehydrogenase E1-alpha (PDHE1α), and of pyruvate dehydrogenase kinase 1 (PDHK1), which catalyzes an inhibitory phosphorylation of PDHC, were unchanged after a one month ketogenic diet (Figure 2 A,E). Levels of CS, a proximal TCA cycle enzyme, and malate dehydrogenase 2 (MDH2), a distal TCA cycle enzyme, were unchanged (Figure 2 B,E). The amount of enolase, a glycolysis enzyme, did not change (Figure 2 C,E).

The level of phosphoenolpyruvate carboxykinase 1 (PEPCK; PCK1), a proximal gluconeogenesis enzyme, was lower in whole cell lysates from ketogenic diet-fed mice (Figure 2 D,E). Because malate dehydrogenase 1 (MDH1) can divert OAA, the PCK1 substrate, from gluconeogenesis we also measured MDH1 levels and these were similar between the groups (Figure 2D,E). The level of fructose-1,6-bisphosphatase 1 (FBP1), which functions at the distal end of the gluconeogenesis pathway, was statistically unchanged ($p=0.11$) although after normalizing to tubulin there was an apparent trend that was opposite in direction to the observed change in PCK1 (Figure 2D,E).

Electron transport chain and MnSOD

MnSOD and a set of electron transport chain subunit levels were assessed only in whole cell lysates, as enriched mitochondria protein samples were not available for these analyses. In all cases densitometry values were normalized to those of tubulin and the resulting normalized values were used to make statistical comparisons.

Fatty acid β-oxidation generates large amounts of NADH, which donate high-energy electrons to NADH-ubiquinone oxidoreductase (complex I) of the electron transport chain; fatty acid β-oxidation also generates large amounts of FADH2 and high energy electrons from FADH2 enter the electron transport chain at succinate dehydrogenase (complex II). Levels of the mitochondrial DNA-encoded complex I subunit NADH-ubiquinone oxidoreductase subunit 1 (MT-ND1) were equivalent between the ketogenic diet and standard chow fed groups (Figure 3A,D). Levels of a nuclear DNA-encoded complex II subunit, succinate dehydrogenase complex subunit A (SDHA), were similarly equivalent (Figure 3A,D). Despite this, levels of two cytochrome c oxidase (COX; complex IV) subunits, the mtDNA-encoded COX subunit II (MT-CO2) and the nuclear DNA-encoded COX subunit 4 isoform 1 (COX4I1), were lower in the ketogenic diet-fed mice (Figure 3B,D). Levels of cytochrome c, a heme protein which delivers electrons to COX, were similarly reduced (Figure 3B,D).

The electron transport chain can directly produce superoxide and through this generate oxidative stress. Mitochondria use manganese superoxide dismutase (MnSOD) to manage electron transport chain-derived superoxide. MnSOD levels were equivalent between the ketogenic and standard chow diet groups (Figure 3C,D).

PGC1α and mitochondrial mass markers

Peroxisome proliferator-activated receptor gamma coactivator 1-alpha (PGC1α) is a transcriptional co-activator that facilitates mitochondrial biogenesis. The whole hepatocyte, tubulin-normalized PGC1α level was lower in mice on the ketogenic diet (Figure 4A,C). Whole hepatocyte, tubulin-normalized levels of two mitochondrial mass markers, the translocase of the outer mitochondrial membrane 20 (TOMM20) and the voltage-dependent anion channel (VDAC) proteins, though, were increased in ketogenic diet-fed mice (Figure 4B,C).

Discussion

The goals of this study were to determine how a ketogenic diet affects representative proteins that mediate various hepatocyte bioenergetic fluxes and also lysine acetylation and succinylation at the hepatocyte proteome level. Some of our findings seem predictable. For example, fatty acid β-oxidation creates relatively large amounts of mitochondrial acetyl CoA, which would expectedly increase mitochondrial protein lysine acetylation. Related findings, such as readily detectable increased whole cell lysine acetylation, are perhaps less obvious and invite speculation. If indeed acetyl groups were transferred from the mitochondria to the cytosol, it would presumably involve export in the form of citrate. To facilitate this, a fatty acid β-oxidation mediated conversion of NAD+ to NADH could have caused a relative inhibition of dehydrogenase-catalyzed TCA cycle steps including the flow of citrate to α-ketoglutarate. A decrease in SIRT3, the major mitochondrial NAD+-dependent deacetylase, might also reflect a lowering of the mitochondrial matrix NAD+/NADH ratio (Rardin et al. 2013a).

Ketone body catabolism requires the transfer of a CoA group from succinyl CoA, a TCA cycle intermediate. Hepatocytes are producers and not consumers of ketone bodies, though, so this would not be expected to impact mitochondrial succinate levels. On the other hand, fatty acid β-oxidation increases FADH2, which could conceivably increase succinate levels by blocking its TCA cycle conversion to fumarate. Independent of succinate levels, though, succinylation does compete with acetylation at some but not all lysines (Park et al. 2013) and this could have prompted changes to the proteome lysine succinylation pattern. An increase in mitochondrial SIRT5, we speculate, could have facilitated the removal of succinate from lysines that can be either succinylated or acetylated, which would indirectly facilitate lysine acetylation. Some of the removed succinates, though, may have in turn increased the succinylation of lysines that are not acetylated. To further place our succinylation and SIRT5 findings within the context of the existing literature, a prior study found eliminating SIRT5 in mice reduced β-hydroxybutyrate production, which was mediated by a subsequent inhibitory succinylation of HMGCS2, the rate limiting enzyme in ketone body synthesis (Rardin et al. 2013b). Presumably, then, an increase in hepatocyte SIRT5 should also be consistent with ketogenic diet-induced ketone body production.

We did not observe a change in the absolute PDHC level, or a change in the amount of PDHK1, a kinase that modifies PDHC activity. PDHC, though, is targeted by SIRT5 and SIRT5-mediated PDHC desuccinylation reduces PDHC activity (Park et al. 2013). This raises the obvious point that failure to detect a change in the amount of an enzyme does not

necessarily mean its activity is not altered. This applies to the hepatocyte TCA and glycolysis protein levels we assessed, whose levels appeared unchanged following completion of a one-month ketogenic diet.

The level of a proximal gluconeogenesis enzyme, PCK1, did decline while the level of a more distal gluconeogenesis enzyme, FBP1, trended higher. Consistent with our PCK1 protein observation, hepatocyte PCK1 mRNA was also found to be reduced in mice on a ketogenic diet (Kennedy et al. 2007). Conceptually, it does make sense that low carbohydrate intake would reduce lactate and pyruvate, and in particular their diversion into gluconeogenesis. However, carbon from other sources, including glycerol, can be used to support gluconeogenesis and this may play a critical role in preventing hypoglycemia during high fat, low carbohydrate ketogenic diets. This could potentially account for why we found PCK1 protein was decreased while the amount of FBP1 protein trended in an upward direction.

A fatty acid β-oxidation fueled increase in mitochondrial matrix NADH and FADH2 might, it seems, place complicated demands on mitochondrial homeostasis. Oxidation of NADH and FADH2 back to NAD+ and FAD should to some extent be accomplished by donation of electrons to complex I (from NADH) and complex II (from FADH2), but in excess this could lead to mitochondrial membrane hyperpolarization and oxidative stress. We wonder if this overall dynamic could account for why the cytochrome c and complex IV subunits we measured, but not the complex I or II protein subunits we measured, were decreased.

Maintaining proper electron transport chain holoenzyme and subunit stoichiometry undoubtedly helps optimize respiration, and our findings indicate in hepatocytes a ketogenic diet altered this stoichiometry. MnSOD levels were unchanged, though, which suggests these stoichiometric changes were primarily adaptive. Interestingly, selectively reducing COX holoenzyme levels via knock-out of COX10, a farnesyltransferase that contributes to heme synthesis, was found to reduce oxidative stress in an Alzheimer's disease mouse model (Fukui et al. 2007). Given the known functional and structural connections between heme, cytochrome c, and COX it is therefore not surprising that a decrease in cytochrome c would accompany a decrease in COX subunits.

Our collective data suggest a ketogenic diet's effects on mitochondrial biogenesis are not simple. Levels of a number of mitochondria-localized proteins we have thus far discussed were unchanged (CS, MDH2, PDHE1α, PDHK1, MT-ND1, SDHA1, MnSOD), some were decreased (MT-CO2, COX4I1, cytochrome c, SIRT3), and some were increased (SIRT5). Levels of the TOMM20 and VDAC proteins, which we specifically measured in order to assess mitochondrial mass increased but on the other hand levels of PGC1α, which facilitates mitochondrial biogenesis, were actually reduced. Limitations in the immunochemical characterization of PGC1α have been raised, which could lead some to question this finding. To some extent, therefore, it is reassuring that levels of some proteins PGC1α is known to facilitate the transcription of, including COX4I1, cytochrome c, and SIRT3, were decreased (Kong et al. 2010; Wu et al. 1999). A synthesis of these data suggests changes in hepatocyte mitochondrial mass were likely strategic, as opposed to indiscriminate and diffuse.

The mice we analyzed originally informed a study of how ketogenic diets affect brain bioenergetic infrastructures (Selfridge et al. 2015). The report from that study documents select physiologic effects of the ketogenic diet intervention. After 1 month, the ketogenic diet-fed mice demonstrated increased plasma β-hydroxybutyrate, weighed less than standard chow-fed mice, and according to the homeostatic assessment of insulin resistance (HOMA-IR) calculation (Matthews et al. 1985) showed evidence of enhanced peripheral insulin sensitivity. Brains from the ketogenic diet-fed mice contained less tumor necrosis factor α (TNFα) mRNA, a finding consistent with other data that indicate ketogenic diets reduce inflammation (Dupuis et al. 2015; Ruskin et al. 2009). We did not observe reduced brain levels of COX subunit proteins, as we found in our liver study. Brain and liver tissue, therefore, respond at least somewhat differently to a ketogenic diet.

In addition to basing interpretations on only changes in levels of proteins our study has other limitations. We only evaluated ketogenic diet responses after one month, and we do not know what the levels of our measured proteins would be with shorter or longer diet durations. Also, for whole cell lysate proteins our statistical analyses used tubulin-normalized protein levels. During the course of this study we observed tubulin provided more consistent inter-group measurements than actin (data not shown), and we wished to avoid using GAPDH because of its role in glycolysis. Nevertheless, although we did not detect inter-group differences in the amount of tubulin it is possible differences below the level of our detection could have affected our calculations and therefore our interpretations. Finally, we interrogated only select components of pathways and multi-subunit proteins which forced us to use partial insight to impute the status of the bioenergetic pathways of interest. Based on all these limitations we wish to emphasize the pilot nature of this study, and that some of our findings are more useful for generating hypotheses than resolving hypotheses. Figure 5 summarizes much of the data generated during the course of this study, and our attempt to use those data to inform a bioenergetics systems overview of how a ketogenic diet influences hepatocyte energy metabolism and proteomes.

Acknowledgments

This project was supported by the University of Kansas Alzheimer's Disease Center (NIH P30 AG035982).

References

Douris N, Melman T, Pecherer JM, Pissios P, Flier JS, Cantley LC, Locasale JW, Maratos-Flier E. Adaptive changes in amino acid metabolism permit normal longevity in mice consuming a low-carbohydrate ketogenic diet. Biochimica et biophysica acta. 2015; 1852(10 Pt A):2056–2065. [PubMed: 26170063]

Dupuis N, Curatolo N, Benoist JF, Auvin S. Ketogenic diet exhibits anti-inflammatory properties. Epilepsia. 2015; 56(7):e95–98. [PubMed: 26011473]

Fukui H, Diaz F, Garcia S, Moraes CT. Cytochrome c oxidase deficiency in neurons decreases both oxidative stress and amyloid formation in a mouse model of Alzheimer's disease. Proc Natl Acad Sci U S A. 2007; 104(35):14163–14168. [PubMed: 17715058]

Halestrap AP, Wilson MC. The monocarboxylate transporter family–role and regulation. IUBMB life. 2012; 64(2):109–119. [PubMed: 22162139]

Holland AM, Kephart WC, Mumford PW, Mobley CB, Lowery RP, Shake JJ, Patel RK, Healy JC, McCullough DJ, Kluess HA, Huggins KW, Kavazis AN, Wilson JM, Roberts MD. Effects of a ketogenic diet on adipose tissue, liver, and serum biomarkers in sedentary rats and rats that

exercised via resisted voluntary wheel running. American journal of physiology Regulatory, integrative and comparative physiology. 2016; 311(2):R337–351.

Jornayvaz FR, Jurczak MJ, Lee HY, Birkenfeld AL, Frederick DW, Zhang D, Zhang XM, Samuel VT, Shulman GI. A high-fat, ketogenic diet causes hepatic insulin resistance in mice, despite increasing energy expenditure and preventing weight gain. American journal of physiology Endocrinology and metabolism. 2010; 299(5):E808–815. [PubMed: 20807839]

Kennedy AR, Pissios P, Otu H, Roberson R, Xue B, Asakura K, Furukawa N, Marino FE, Liu FF, Kahn BB, Libermann TA, Maratos-Flier E. A high-fat, ketogenic diet induces a unique metabolic state in mice. Am J Physiol Endocrinol Metab. 2007; 292(6):E1724–1739. [PubMed: 17299079]

Kong X, Wang R, Xue Y, Liu X, Zhang H, Chen Y, Fang F, Chang Y. Sirtuin 3, a new target of PGC-1alpha, plays an important role in the suppression of ROS and mitochondrial biogenesis. PLoS One. 2010; 5(7):e11707. [PubMed: 20661474]

Krebs HA, Wallace PG, Hems R, Freedland RA. Rates of ketone-body formation in the perfused rat liver. The Biochemical journal. 1969; 112(5):595–600. [PubMed: 5822063]

Lehninger AL, Sudduth HC, Wise JB. D-beta-Hydroxybutyric dehydrogenase of muitochondria. The Journal of biological chemistry. 1960; 235:2450–2455. [PubMed: 14415394]

Manninen AH. Metabolic effects of the very-low-carbohydrate diets: misunderstood “villains” of human metabolism. Journal of the International Society of Sports Nutrition. 2004; 1(2):7–11. [PubMed: 18500949]

Matthews DR, Hosker JP, Rudenski AS, Naylor BA, Treacher DF, Turner RC. Homeostasis model assessment: insulin resistance and beta-cell function from fasting plasma glucose and insulin concentrations in man. Diabetologia. 1985; 28(7):412–419. [PubMed: 3899825]

McDaniel SS, Rensing NR, Thio LL, Yamada KA, Wong M. The ketogenic diet inhibits the mammalian target of rapamycin (mTOR) pathway. Epilepsia. 2011; 52(3):e7–11. [PubMed: 21371020]

Murata Y, Nishio K, Mochiyama T, Konishi M, Shimada M, Ohta H, Itoh N. Fgf21 impairs adipocyte insulin sensitivity in mice fed a low-carbohydrate, high-fat ketogenic diet. PloS one. 2013; 8(7):e69330. [PubMed: 23874946]

Newman JC, Verdin E. Ketone bodies as signaling metabolites. Trends in endocrinology and metabolism: TEM. 2014; 25(1):42–52. [PubMed: 24140022]

Okuda T, Fukui A, Morita N. Altered expression of O-GlcNAc-modified proteins in a mouse model whose glycemic status is controlled by a low carbohydrate ketogenic diet. Glycoconjugate journal. 2013; 30(8):781–789. [PubMed: 23793825]

Park J, Chen Y, Tishkoff DX, Peng C, Tan M, Dai L, Xie Z, Zhang Y, Zwaans BM, Skinner ME, Lombard DB, Zhao Y. SIRT5-mediated lysine desuccinylation impacts diverse metabolic pathways. Molecular cell. 2013; 50(6):919–930. [PubMed: 23806337]

Puchalska P, Crawford PA. Multi-dimensional Roles of Ketone Bodies in Fuel Metabolism, Signaling, and Therapeutics. Cell metabolism. 2017; 25(2):262–284. [PubMed: 28178565]

Rardin MJ, Newman JC, Held JM, Cusack MP, Sorensen DJ, Li B, Schilling B, Mooney SD, Kahn CR, Verdin E, Gibson BW. Label-free quantitative proteomics of the lysine acetylome in mitochondria identifies substrates of SIRT3 in metabolic pathways. Proc Natl Acad Sci U S A. 2013a; 110(16):6601–6606. [PubMed: 23576753]

Rardin MJ, He W, Nishida Y, Newman JC, Carrico C, Danielson SR, Guo A, Gut P, Sahu AK, Li B, Uppala R, Fitch M, Riiff T, Zhu L, Zhou J, Mulhern D, Stevens RD, Ilkayeva OR, Newgard CB, Jacobson MP, Hellerstein M, Goetzman ES, Gibson BW, Verdin E. SIRT5 regulates the mitochondrial lysine succinylome and metabolic networks. Cell metabolism. 2013b; 18(6):920–933. [PubMed: 24315375]

Ruskin DN, Kawamura M, Masino SA. Reduced pain and inflammation in juvenile and adult rats fed a ketogenic diet. PloS one. 2009; 4(12):e8349. [PubMed: 20041135]

Selfridge JE, Wilkins HM, E L, Carl SM, Koppel S, Funk E, Fields T, Lu J, Tang EP, Slawson C, Wang W, Zhu H, Swerdlow RH. Effect of one month duration ketogenic and non-ketogenic high fat diets on mouse brain bioenergetic infrastructure. J Bioenerg Biomembr. 2015; 47(1-2):1–11. [PubMed: 25104046]

Swerdlow RH. Bioenergetic medicine. Br J Pharmacol. 2014; 171(8):1854–1869. [PubMed: 24004341]

Wu Z, Puigserver P, Andersson U, Zhang C, Adelmant G, Mootha V, Troy A, Cinti S, Lowell B, Scarpulla RC, Spiegelman BM. Mechanisms controlling mitochondrial biogenesis and respiration through the thermogenic coactivator PGC-1. Cell. 1999; 98(1):115–124. [PubMed: 10412986]

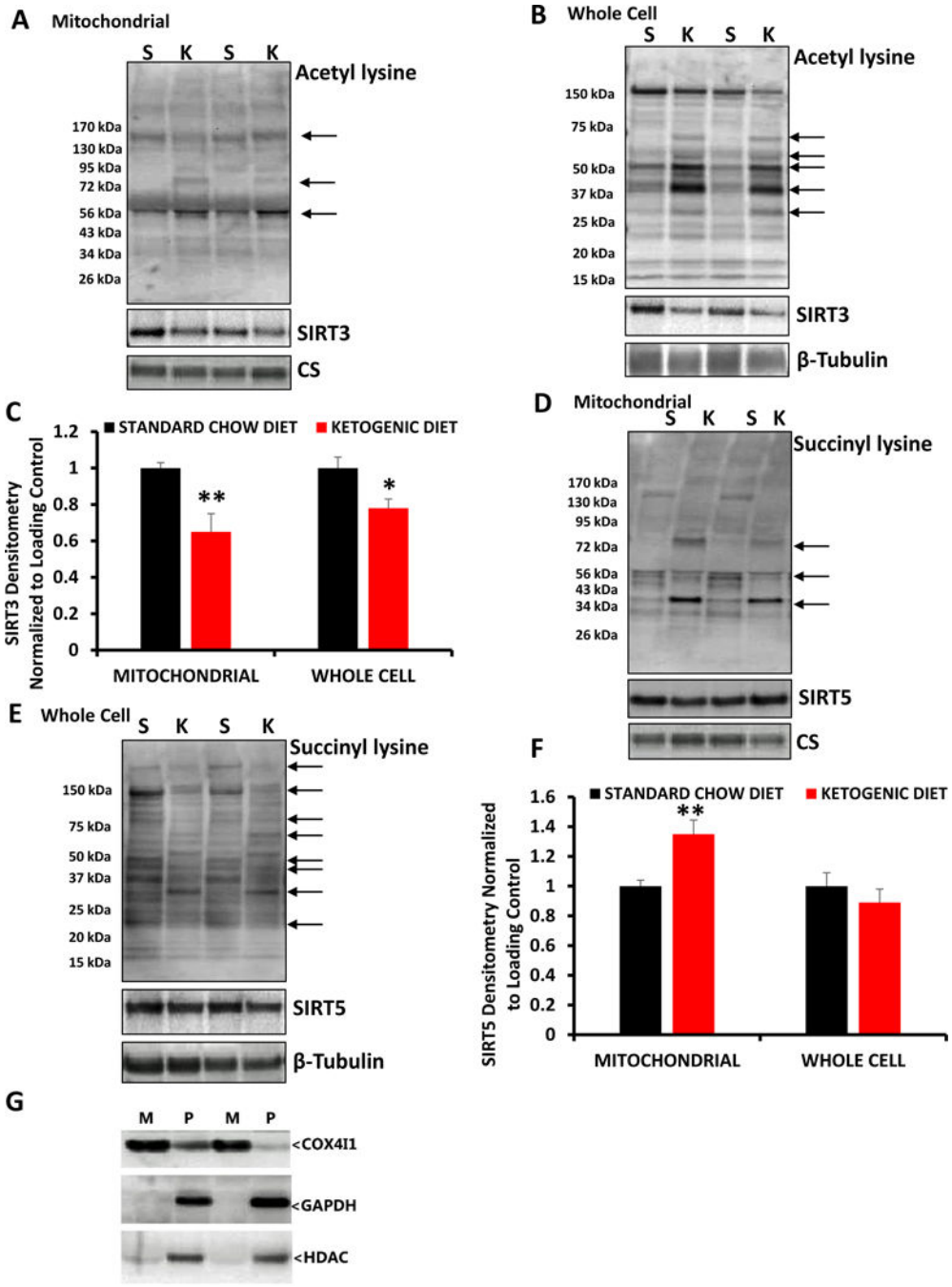

Figure 1. Proteome acetylation and succinylation, SIRT3, and SIRT5

A. Representative blots illustrating the degree of mitochondrial enrichment and purification that were achieved, in which COX4I1 (a mitochondrial protein) demonstrates mitochondrial lysate enrichment, and GAPDH (a cytosolic protein) and HDAC (a nuclear protein) demonstrate mitochondrial lysate purity. **B.** Liver mitochondria-enriched lysates were immunoblotted against acetyl lysine, SIRT3, and CS (representative blots). **C.** Liver whole cell lysates were immunoblotted against acetyl lysine, SIRT3, and β-tubulin (representative blots). **D.** Densitometry analysis of mitochondrial and whole cell SIRT3. **E.** Liver

mitochondria-enriched lysates were immunoblotted against succinyl lysine, SIRT5, and CS (representative blots). **F.** Liver whole cell lysates were immunoblotted against succinyl lysine, SIRT5, and β-tubulin (representative blots). Data are shown as means +/−SEM. *$p < 0.05$, **$p < 0.01$. S=standard chow diet, K=ketogenic diet, M=mitochondrial lysate, WC=whole cell lysate. Arrows indicate differences in post-translational modifications between groups. n=15 for the ketogenic diet analyses, and n=11 for the standard chow analyses.

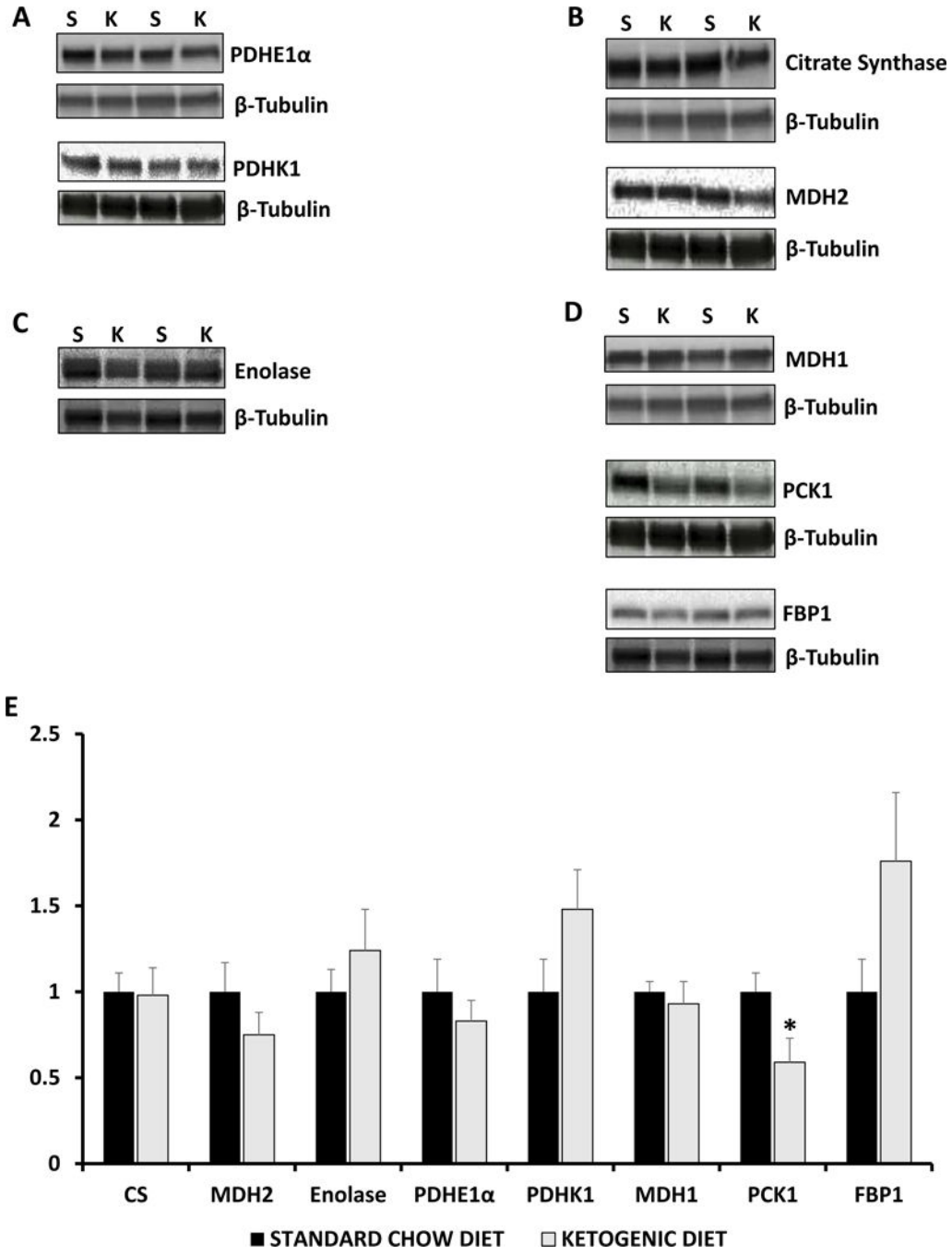

Figure 2. PDHC/PDHK1 and TCA cycle, glycolysis, and gluconeogenesis enzymes

Liver whole cell lysates were immunoblotted against **A.** PDH1Eα, PDHK1, and β-tubulin (representative blots); **B.** CS, MDH2, and β-tubulin (representative blots); **C.** enolase and β-tubulin (representative blots); and **D.** MDH1, PCK1, FBP1, and β-tubulin (representative blots). **E.** Densitometry analysis of PDH1Eα, PDHK1, CS, MDH2, enolase, MDH1, PCK1 and FBP1. Data are shown as means +/−SEM. *$p < 0.05$. S=standard chow diet, K=ketogenic diet. n=15 for the ketogenic diet analyses, and n=11 for the standard chow analyses.

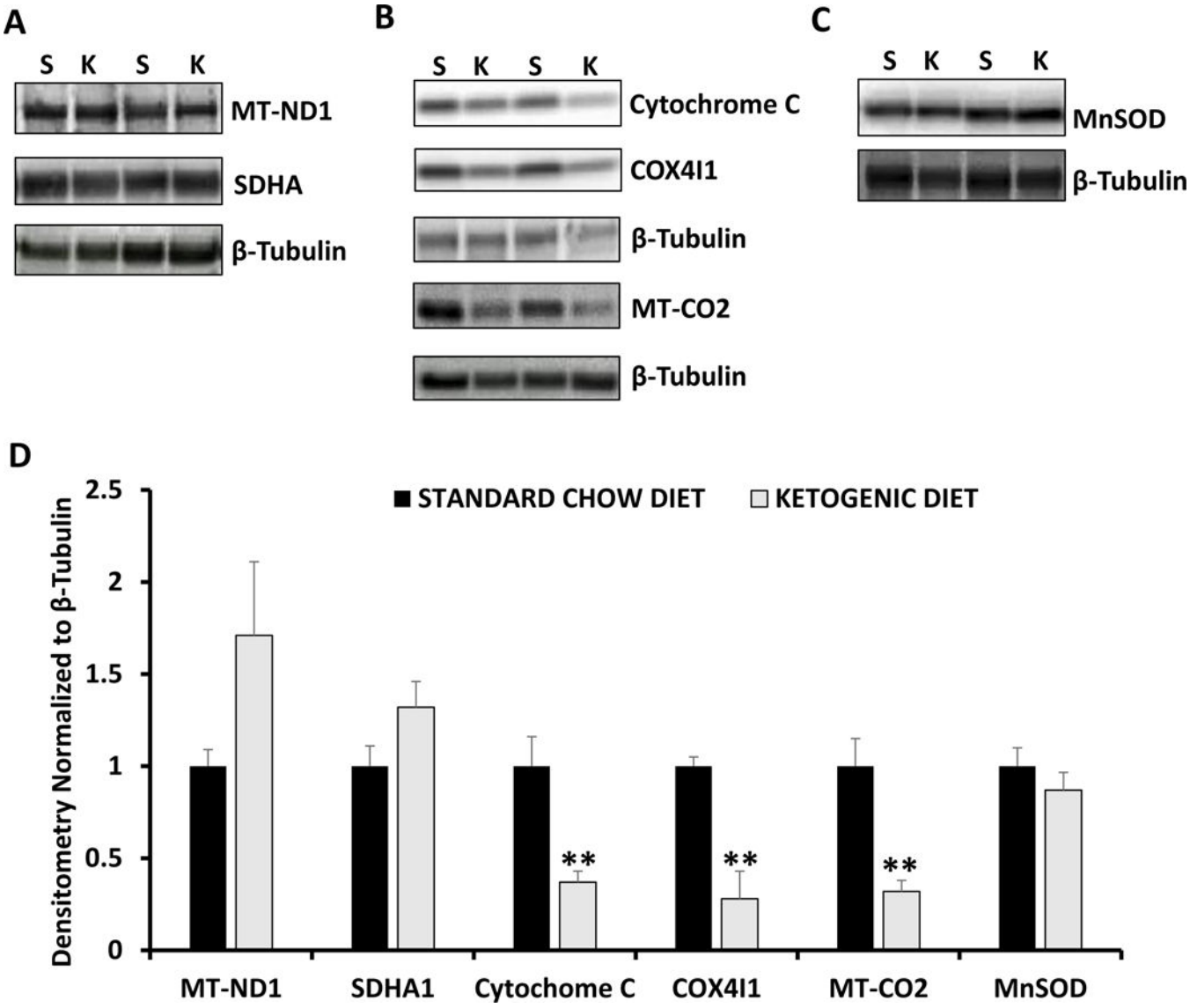

Figure 3. Electron transport chain and MnSOD

Liver whole cell lysates were immunoblotted against **A.** MT-ND1, SDHA, and β-tubulin (representative blots); **B.** cytochrome C, COX4I1, MT-CO2, and β-tubulin (representative blots); and **C.** MnSOD and β-tubulin (representative blots). **D.** Densitometry analysis of MT-ND1, SDHA, cytochrome C, COX4I1, MT-CO2, and MnSOD. Data are shown as means +/−SEM. **p < 0.01. S=standard chow diet, K=ketogenic diet. n=15 for the ketogenic diet analyses, and n=11 for the standard chow analyses.

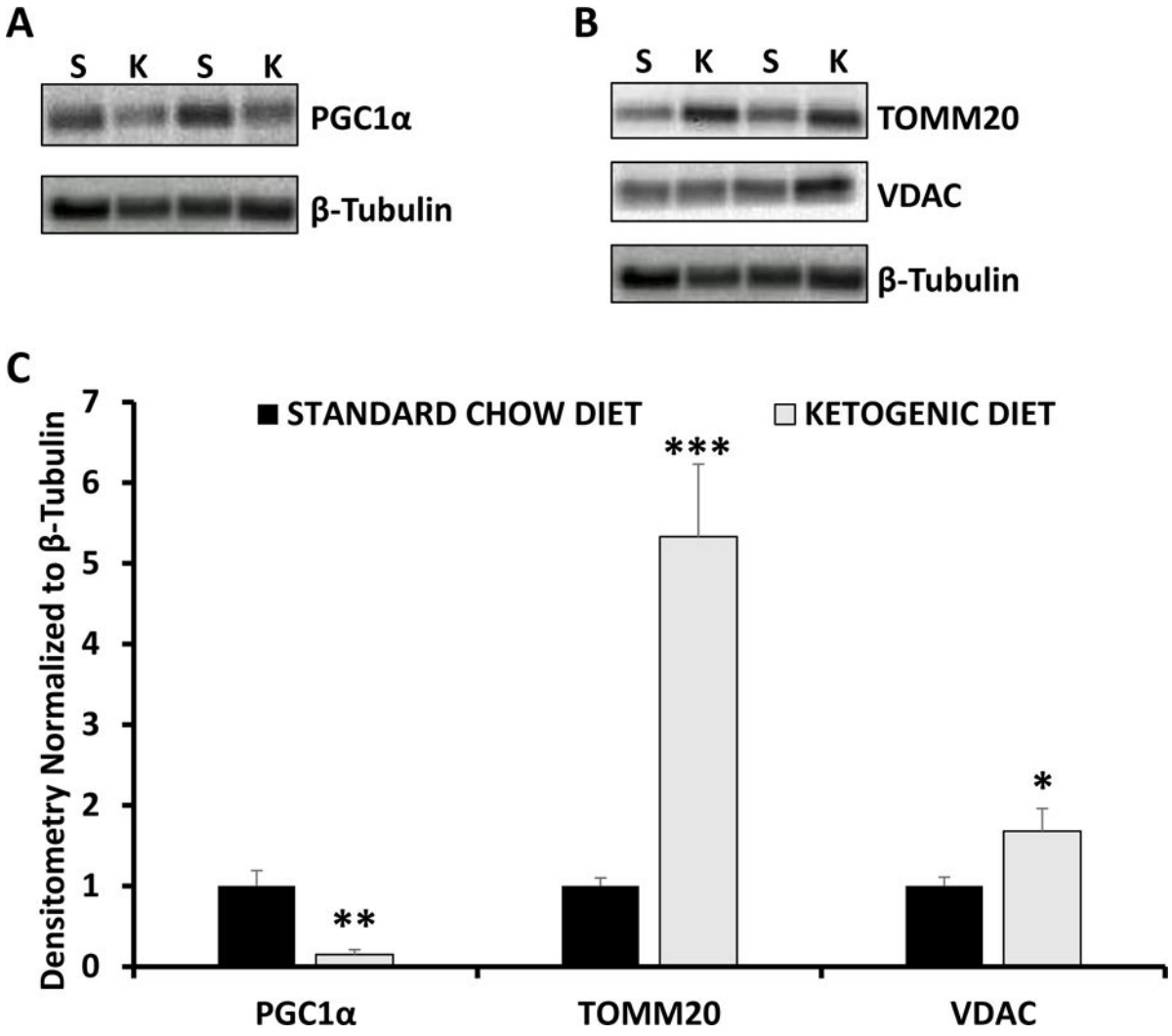

Figure 4. PGC1α and mitochondrial mass markers

Liver whole cell lysates were immunoblotted against **A.** PGC1α and β-tubulin (representative blots), and **B.** TOMM20, VDAC, and β-tubulin (representative blots). **C.** Densitometry analysis of PGC1α, TOMM20, and VDAC. Data are shown as means +/−SEM. *p < 0.05, **p < 0.01, ***p < 0.001. S=standard chow diet, K=ketogenic diet. n=15 for the ketogenic diet analyses, and n=11 for the standard chow analyses.

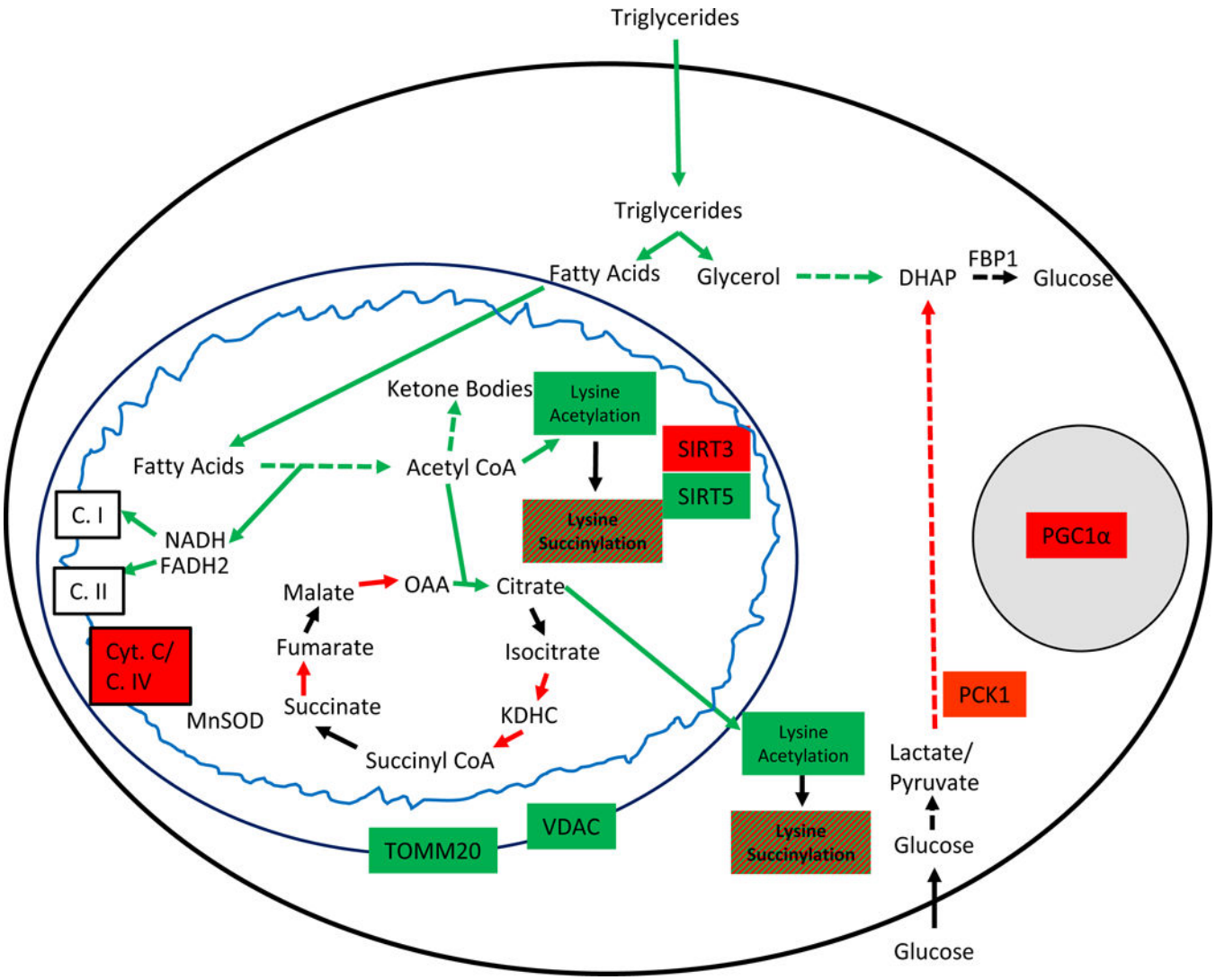

Figure 5. Bioenergetic systems overview of ketogenic diet hepatocyte effects

The large oval represents a cell, with a mitochondrion (with an outer and inner membrane) located on the left and a nucleus (shown in gray) on the right. Proteins whose levels were observed to increase are shown with a green background, while proteins whose levels were observed to decrease are shown with a red background. Lysine succinylation total levels did not grossly change although the banding pattern did change; lysine succinylation is indicated using a red-green striped background. Fluxes for some pathways, including fatty acid β-oxidation, ketogenesis, gluconeogenesis, and the TCA cycle were inferred based on our observed results as well as data from existing studies; red arrows assume a flux decrease, green arrows predict a flux increase, and black arrows indicate no flux assumption is offered. Dashed arrows indicate multiple steps are involved. C. I=complex I, C. II=complex II, C. IV=complex IV, Cyt. C=cytochrome c.

Table 1

Antibodies

Immunogen	Company
Acetyl Lysine	Abcam #ab21623
β-Tubulin	Abcam #ab6046
Citrate Synthase (CS)	Cell signaling #D7V8B
Cytochrome C	Cell Signaling #D18C7
Cytochrome oxidase subunit 4 isoform 1 (COX4I1)	Cell Signaling #48445
Cytochrome C oxidase subunit II (MT-CO2)	Abcam #ab79393
Enolase-1	Cell Signaling #38105
Fructose-1,6-bisphosphatase (FBP1)	Abcam #ab109020
Glyceraldehyde 3-phosphate (GAPDH)	Cell Signaling #D16H11
Histone Deactyelase 1 (HDAC)	Cell Signaling #10E2
Malate dehydrogenase 1 (MDH1)	Abcam #ab180152
Malate dehydrogenase 2 (MDH2)	Cell Signaling #D8Q5S
Manganese superoxide dismutase (MnSOD)	BD #611580
NADH-ubiquinone oxidoreductase chain 1 (MT-ND1)	Abcam #ab74257
Peroxisome proliferator-activated receptor gamma coactivator 1-alpha (PGC1α)	Abcam #ab191838
Phosphoenolpyruvate carboxykinase 1 (PCK1)	Abcam #70358
Pyruvate dehydrogenase E1-alpha subunit (PDHE1α)	Abcam #ab92696
Pyruvate dehydrogenase kinase 1 (PDHK1)	Cell Signaling #C47H1
Succinate dehydrogenase complex subunit A (SDHA)	Abcam #ab14715
SIRT3	Cell Signaling #D22A3
SIRT5	Cell Signaling #D5E11
Succinyl Lysine	PTM Biolabs #PTM-401
Translocase of the outer mitochondrial membrane 20 (TOMM20)	Santa Cruz #sc-136211
Voltage dependent anion channel (VDAC)	Cell Signaling #4866